Rutherford and Appleton Laboratories
CHILTON, DIDCOT, OXON, OX11 0QX

New Equations of State for Medusa

A R Bell

RL-80-091
Copy 1

December 1980

NEW EQUATIONS OF STATE FOR MEDUSA

A R Bell

SRC Rutherford & Appleton Laboratories, Chilton, Didcot,
Oxfordshire, UK.

Abstract

Three new options for the equation of state have been added to the Medusa computer simulation of laser-driven compression of matter. They are based on the Thomas-Fermi model of atomic structure. The first option is a set of analytic approximations to graphs of the Thomas-Fermi pressure and energy as functions of temperature and atomic volume prepared by Latter (1955). The second option includes quantum and exchange corrections to the degeneracy pressure and energy (Kirznitz, 1959) which model a condensed phase. The third option is a variation on the second option which allows the density of the condensed phase to be adjusted to agree with the measured value.

(1) Introduction

Medusa (Christiansen et al., 1974) is a computer program which is widely used to simulate the compression of inertially confined fusion targets by laser irradiation. The program calculates pressure and energy as sums of the electron and ion pressures and energies. The ions are treated as a perfect gas. The electrons are described either by the perfect gas (PG) or Fermi-Dirac (FD) equations of state. Recent laser-compression experiments have operated in ablative mode for which these equations of of state are not always adequate. The FD equation of state is accurate at high temperatures and pressures but cannot model the relatively low pressures which occur near solid density in low entropy ablative implosions. For example it gives a degeneracy pressure of the order of 10 Mbar at solid densities which is orders of magnitude greater than the real pressure. We report here on new options which we have developed for the electron equation of state in Medusa. Our aim has been to produce alternative equations of state which are easy to use, do not take a large amount of computer time, but yet are a significant improvement on previous equations of state. We have developed analytic approximations to the Thomas-Fermi (TF) and corrected-Thomas-Fermi (TFC) equations. For discussions of these equations of state the reader is referred to reviews by March (1955), Brush (1967), and Kirznitz et al. (1976). Our routines have been in use for a year and have recently been updated and some of the equations changed to make it easier for the inexperienced user to run Medusa without having to involve himself in the details of the equation of state.

(2) The Thomas-Fermi equation of state

The Thomas-Fermi (TF) theory is a quantum-statistical model of the electron distribution surrounding atomic nuclei. It includes degeneracy pressure and the effect on the electron distribution of the potential well around the electron-shielded nucleus. In contrast to the Fermi-Dirac (FD) theory which ignores the nuclear potential, electrons congregate around the nucleus at low temperature thus modelling recombination and reducing the electron pressure.

Graphs of the Thomas-Fermi pressure and energy density as functions of density and temperature were published by Latter (1955) and we have constructed the analytic approximations given below to fit his curves. V is the volume occupied by one atom, and U is the energy of one atom. The expressions are correct for a hydrogen plasma and can be put in the appropriate form for other elements by substituting Z*V for V, T*Z**(-4./3.) for T, P*Z**(-10./3.) for P, and U*Z**(-7./3.) for U, where Z is the nuclear charge. The units are cgs apart from energy and temperature which are in eV. The values of the numerical constants are tabulated in the appendix. The expressions for the energy and pressure degeneracy curves are taken from March (1955).

Pressure

```
P1=1.602E-12*T/V
     5
P2=(ΣA(N)*V**(N/6.+0.5))**-2.5
    N=1
P3=(1./V-0.75E-18*V**-1.75)*(P4**-2.+P5**-2.)**-0.5

   +0.75E-18*V**-1.75*P5

     where P4=A6*T and P5=A7*T**1.61
```

The TF pressure is then given by

```
PTF=0.2*P1+P2+0.8*P3
```

Energy

```
U1=1.5*T

U2=A10*AD+A11*SQRT(XO)*PHI**2.5
                                7
     where AD=1./(BO*XO**7.772+ΣB(K)*XO**K)
                  6           K=1
           PHI=1./(ΣC(K)*XO**(K/2.))
                  K=1
           XO=1.324E8*V**0.33333333

U3=(1.E-18*V**-0.75+ALOG(V*1.E22))*(A12*T**0.1466+A13*T**-1.0733)**-1.5

U4=1.5*T*T/(1.1+T)
```

The TF energy is given by

```
UTF = 0.2*U1 + U2 + 0.8*(U3 + U4)
```

Energy derivatives

a) Temperature

```
DUT1=1.5

DUT3=(1.E-18*V**-0.75+ALOG(V*1.E22))*(1.61*A13*T**-2.0733333-

     0.22*A12*T**-0.853333)*(A12*T**0.146666+A13*T**-1.073333)**-2.5

DUT4=1.5*T*(2.2+T)*(1.1+T)**-2.
```

The temperature derivative of the electron energy for one atom is given by

```
DUDT = 0.2*DUT1 + 0.8*(DUT3+DUT4)
```

b) Volume

```
DUV3=(1./V-0.75E-18*V**-1.75)*(A12*T**.14666+A13*T**-1.07333)**-2.5
```

The sum of the pressure and the volume energy derivative in cgs units is

```
P+dU/dV = 0.8*DUV3 + 0.2*P1 + 0.8*P2
```

These approximations preserve the required thermodynamic relationship between pressure and energy.

```
dU/dV = T*(dP/dT) - P
```

Pressure and energy for the exact TF equation of state and our analytic approximations are plotted in Fig. 1 to Fig 4. Fig. 5 and 6 are plots of the errors in the analytic approximations at temperatures between 0.01eV and 10 KeV. At temperatures of 0.1 and 0.01 eV the approximations are inaccurate. However, this is not considered important because the pressures and energies are low compared with those in the implosion, and hence the inaccuracies do not invalidate the simulation. Moreover, the TF model is no longer valid in this regime. While the approximations have been chosen to avoid unphysical results, the main emphasis in the low temperature non-degenerate regime has been to avoid negative specific heats and to maintain a reasonable ratio between pressure and energy density. The approximations used prior to their recent revision sometimes produce negative specific heats and unrealistic ratios of pressure to energy density in the low temperature regime resulting in failure of the program to converge. It is believed that these problems

have now been remedied.

In the more important regime of temperatures greater than 1eV the largest inaccuracies occur when the electrons are partially degenerate. This is where the equations for the degenerate and non-degenerate regimes are joined. The accuracy in the partially degenerate regime could be improved but the analytic approximations would be much more complex with a consequent increase in computing time. At very high temperatures, 1 KeV and above, the equations become those for a perfect gas when the electrons are non-degenerate.

(3) The corrected-Thomas-Fermi (TFC) equation

The Thomas-Fermi equation of state includes only the very basic quantum effect of the Pauli exclusion principle. Further quantum effects can be included by expansion of the Hartree-Fock equation as a series of progressively higher order quantum terms (Brush, 1967). Retaining the first-order terms produces the corrected-Thomas-Fermi (TFC) equation of state (Kirznitz, 1959) in which exchange effects are included. These act as a binding force and the pressure in this approximation can become negative thus modelling a condensed phase. The major advantages for simulation are the more realistic pressures and energies around solid density. Whereas the TF pressure at solid densities is of the order of 1 Mbar, which is an improvement on the 10 Mbar given by the FD equation, the TFC equation gives pressures much less than this, thus avoiding unrealistic initial expansion of the shell material as soon as the laser pulse begins.

The zero temperature part of the Thomas-Fermi corrections can be separated from the temperature-dependent part, and the new Medusa options include only the zero temperature degeneracy corrections. The version in use before the recent update also included the non-zero temperature part but it was found that the approximations could result in a negative specific heat when the corrections dominated causing the calculation to terminate. Retaining only the zero temperature term does not lead to large errors since the corrections are only important at low temperatures. In the regime where the corrections are comparable with the basic TF terms, the model of the atom is inaccurate. Our criterion for use of the model is not theoretical validity, but increased accuracy in the equation of state, and it is therefore consistent with our approach to use only the zero temperature term of the corrections.

The Thomas-Fermi corrections have been tabulated by McCarthy (1965) and Kalitkin (1960) and their data for the correction to the degeneracy pressure has been fitted by the following expression.

```
PCORR=(A8*V**.6645+A9*V**1.185)**-2.
```

The Z scaling of the TFC corrections is different from that of the basic TF pressure and energy, and the Z dependence can be obtained by substituting PCORR*Z**(-8./3.) for PCORR and UCORR*Z**(-5./3.) for UCORR. T and V still scale in the usual way. The subroutine calculating the energy is not called as frequently as the pressure subroutine and for the energy correction we have used an interpolation routine with tables compiled from the data given by McCarthy and Kalitkin instead of fitting an analytic expression. Ignoring the temperature dependent terms, dU/dT and (p+dU/dV) are identically zero for the corrections.

The energy and pressure corrections given by the TFC model are plotted in Fig. 7 to 10 and the errors in the approximations and the neglect of the non-zero temperature part are plotted in Fig. 11 and 12.

The non-zero temperature terms are still available for use if required. In most cases they can be used without causing a failure to converge if a starting temperature of around 1 eV is specified. The starting temperature may have to be increased further for high Z materials. Convergence problems arise if the temperature falls far below that at which the material is partially degenerate.

The sound speed given by the TFC equation of state can depart a long way from $(P/\rho)^{\frac{1}{2}}$ since $dP/d\rho$ is large near solid density. A lower limit of 1.E4*Z**0.666667 m s^{-1} has therefore been applied in the routine TIMSTP which determines the timestep. Some other changes to this subroutine have been made and it was found advisable to place a lower limit of around 1.E-16 on the timestep.

(4) Adjustments to the TFC model

A disadvantage with the TFC equation of state is that the solid-liquid density given by the model does not match the measured value in general.

The density of the condensed phase is a function of Z (Fig. 13) and smooths through the peaks and troughs which occur in the plot of solid density against Z for real elements. The equation of state is also used for compound materials in which case the mean Z for the compound is used in the model. To provide the flexibility needed to start the program at the required solid density a third option (TFCC) has been created in which the magnitude of the correction terms in the TFC model is multiplied by a free parameter f to adjust the solid density. f is chosen such that the combined electron and ion pressure is 100 Kbar at the required solid density and initial temperature.

(5) Comparison with real equations of state

The justification for implementing these options for the equation of state is one of increased accuracy when compared with the experimentally determined equations of state. Fig. 14 to 16 compare the FD, TF and TFC options for the pressure with the best available data for aluminium illustrating a considerable improvement in accuracy. Our best available data is taken from the Sesame library data prepared at Los Alamos (Bennett et al., 1978). The TFC solid density for aluminium is very close to the measured value. Fig. 17 shows pressure data for deuterium. Here, the TFC solid density is in error and Fig. 18 shows the TFCC pressure in which the free parameter f is chosen to produce a better fit.

(6) Postscript to the user

The options described here are intended to be useful for material of any Z, whether an element or compound, and to be used over a very large regime in which solid-liquid binding forces, degeneracy, and ionisation are all important. Our equations of state have limitations both in the validity of the Thomas-Fermi model and in the accuracy of the approximations to the exact equations. Nevertheless, the options we have included in Medusa are a considerable improvement on those previously available.

Steps have been taken to ensure that the new options do not cause convergence problems in Medusa. If however the user finds that the new options result in failure to converge we would be pleased to be informed of the problem.

Appendix

A(1) = 4.486E10

A(2) = 0.

A(3) = 8.5383E17

A(4) = 1.3811E21

A(5) = 5.5707E24

A6 = 1.585E-12

A7 = 6.760E-13

A8 = 3.333E9

A9 = 7.627E20

A10 = 13.172

A11 = 1.7562

A12 = 3.283E7

A13 = 1.805E8

B0 = 1.5311E-6

B(1) = 0.

B(2) = 0.48075

B(3) = 0.43462

B(4) = 6.92013E-2

B(5) = 5.9472E-2

B(6) = -4.9688E-3

B(7) = 4.3386E-4

C(1) = 0.

C(2) = 0.48075

C(3) = 0.

C(4) = 0.06934

C(5) = 9.7E-3

C(6) = 3.3704E-3

References

Bennett B I, Johnson J D, Kerley G I and Rood G T, Los Alamos Lab. report LA 7130 (1978)

Brush S G, Progress in High Temperature Physics and Chemistry, 1, 5 (1967)

Christiansen J P, Ashby D E T F and Roberts K V, Comp Phys Comm, 7, 271 (1974)

Kalitkin N N, Sov Phys JETP, 11, 1106 (1960)

Kirzhnits D A, Sov Phys JETP, 8, 1081 (1959)

Kirzhnits D A, Lozovik Yu E and Shpatakovskaya G V, Sov Phys Usp, 18, 9 (1976)

Latter R, Phys Rev, 99, 1854 (1955)

March N H, Adv Phys, 6, 1 (1955)

McCarthy S L, Lawrence Radiation Lab report UCRL 14364 (1965)

Figure Captions

Fig. 1 Analytic approximations to the electron pressure P*Z**(-10./3.) as a function of Z*V at temperatures T*Z**(-4./3.) between 0.01 eV and 10 KeV. P and V are in cgs units.

Fig. 2 McCarthy's tabulated values of P*Z**(-10./3.) as a function of Z*V at different temperatures.

Fig. 3 Analytic approximations to energy U*Z**(-7./3.) of the Z electrons associated with one nucleus as a function of Z*V at different temperatures. U is in eV.

Fig. 4 McCarthy's tabulated values of U*Z**(-7./3.) as a function of Z*V at different temperatures.

Fig. 5 Graphs of $\Delta P/P_{TF}$ against Z*V at temperatures T*Z**(-4./3.) between 0.01 eV and 10 KeV. P_{TF} is the Thomas-Fermi pressure tabulated by McCarthy. ΔP is the error in the analytic approximation for pressure $\Delta P = P_{APPROX} - P_{TF}$.

Fig. 6 As for Fig. 5 but for energy instead of pressure.

Fig. 7 Analytic approximation to the TFC correction P_c*Z**(-8./3.) to the degeneracy pressure as a function of Z*V.

Fig. 8 McCarthy's tabulated values of the TFC correction P_c*Z**(-8./3.) to the pressure as a function of Z*V at temperatures T*Z**(-4./3.) between 0.01 eV and 10 KeV.

Fig. 9 TFC corrections U_c*Z**(-5./3.) to the energy of the degenerate electrons as tabulated by Kirznitz and incorporated into Medusa.

Fig. 10 McCarthy's tabulated values of the TFC energy corrections mod(U_c*Z**(-5./3.)) as a function of Z*V.

Fig. 11 Graphs of (ΔP_c*Z**(-8./3.))/(P_{TF}*Z**(-10./3.)) against Z*V at different temperatures. P_{TF} is the Thomas-Fermi pressure as

tabulated by McCarthy. ΔP_c is the difference between our approximation to the TFC corrections to the degeneracy pressure and the full temperature dependent corrections tabulated by McCarthy. Thus, ΔP_c includes both the error in our approximation and the error introduced by neglecting the temperature dependent part.

Fig. 12 As for Fig. 11 but for energy instead of pressure.

Fig. 13 Plot of the volume occupied by one atom of an element according to the TFC model as a function of Z. The measured atomic volumes are plotted for comparison.

Fig. 14 Graph of pressure against density for aluminium (solid lines) as given by the FD model, and compared with accurate data from the Sesame library (dotted lines).

Fig. 15 Graph of pressure against density for aluminium as given by the TF model and compared with the Sesame data.

Fig. 16 Graph of pressure against density for aluminium as given by the TFC model and compared with the Sesame data.

Fig. 17 Graph of pressure against density for deuterium as given by the TFC model and compared with the Sesame data.

Fig. 18 Graph of pressure against density for deuterium with the magnitude of the Thomas-Fermi corrections adjusted (TFCC model) to give a better fit to the solid density.

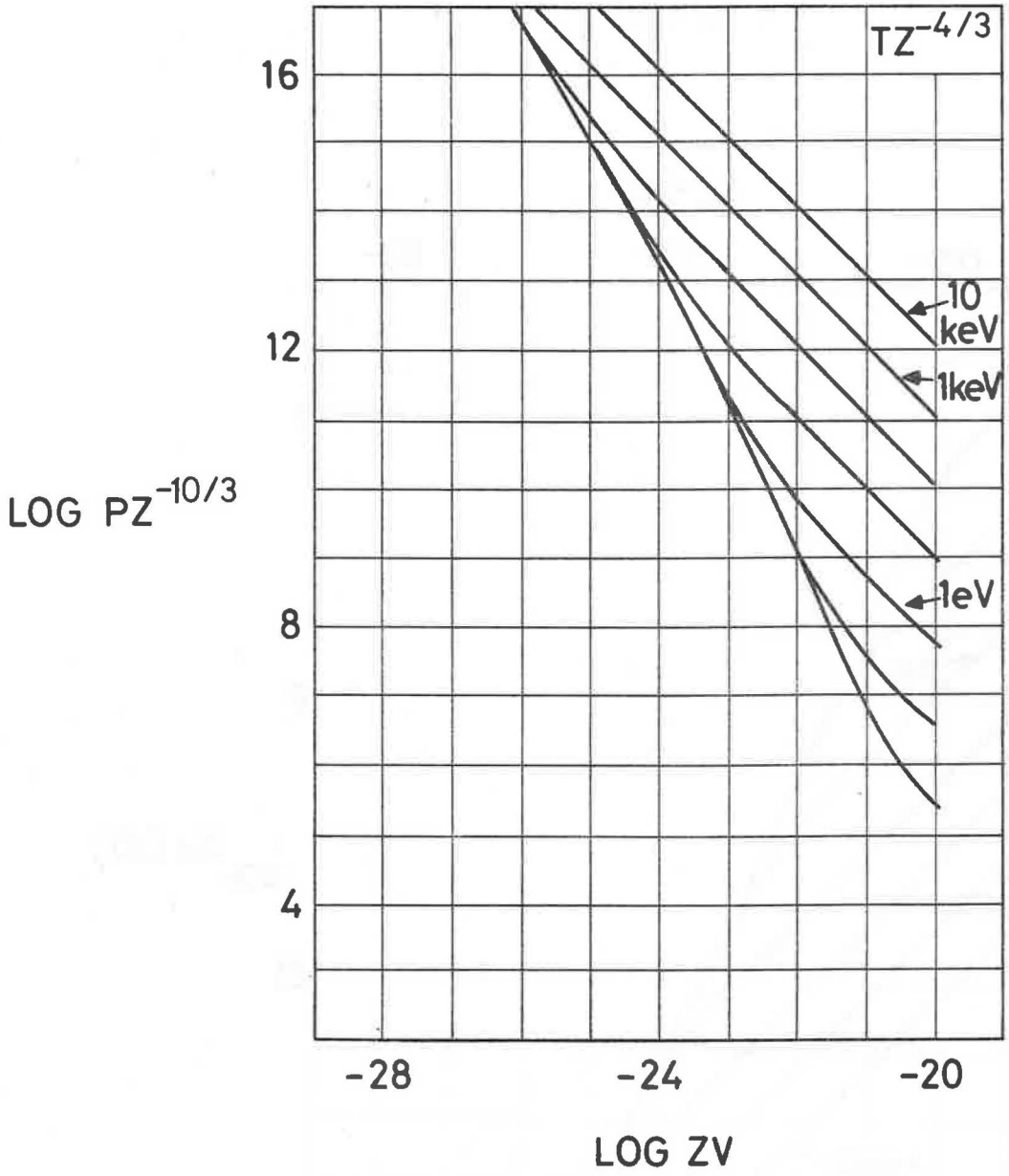

FIG. 1

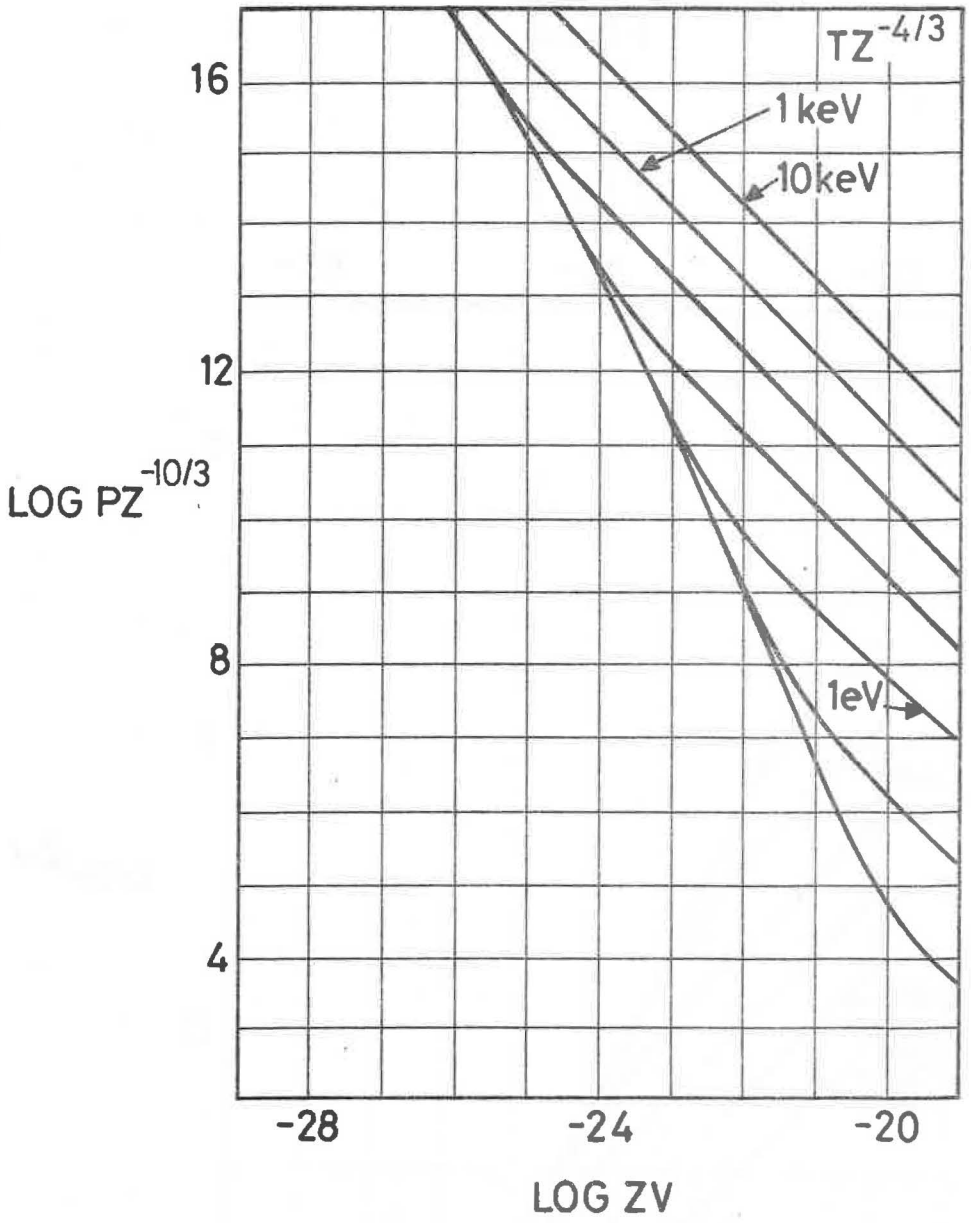

FIG. 2.

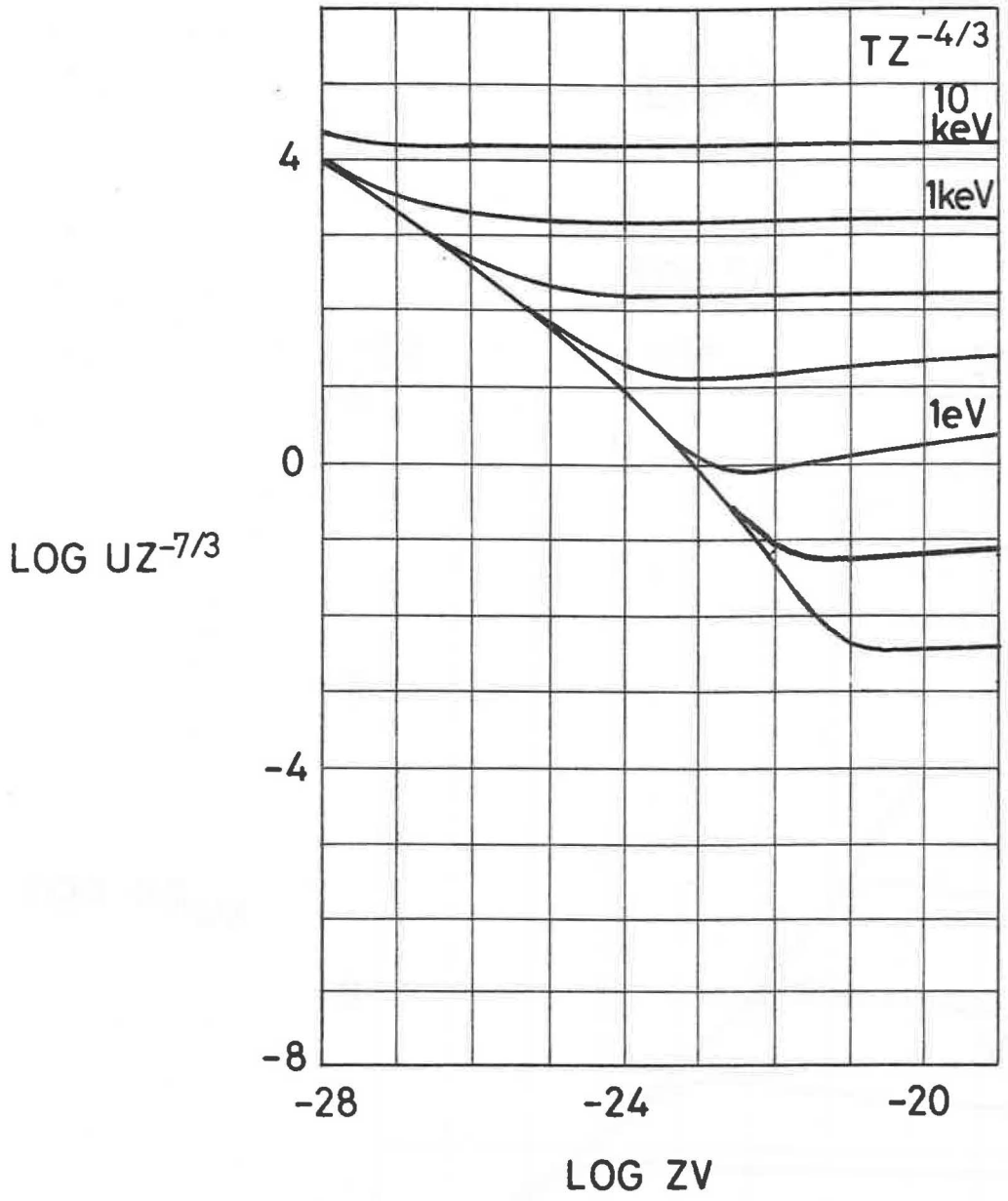

FIG. 3

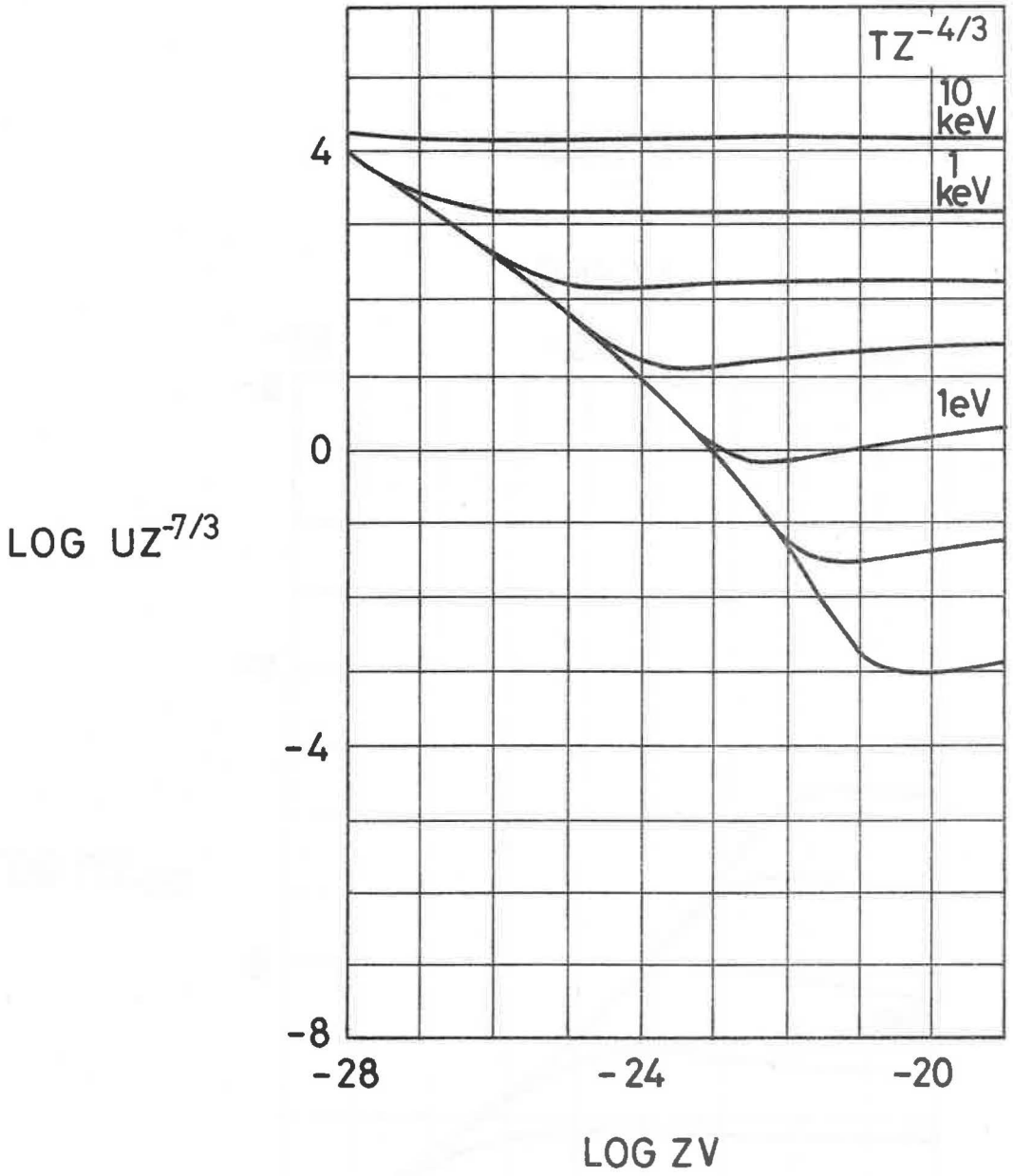

FIG. 4

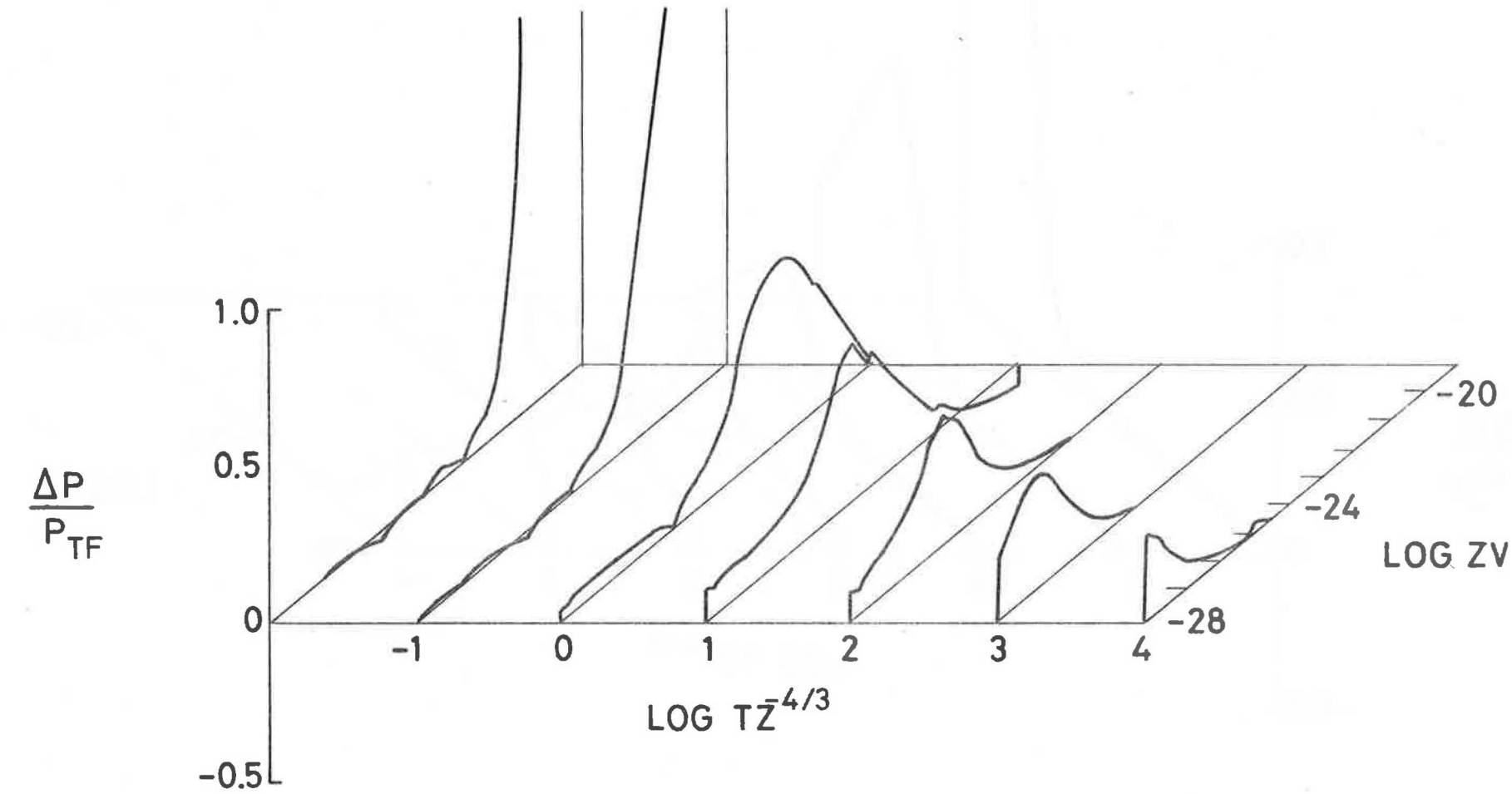

FIG. 5

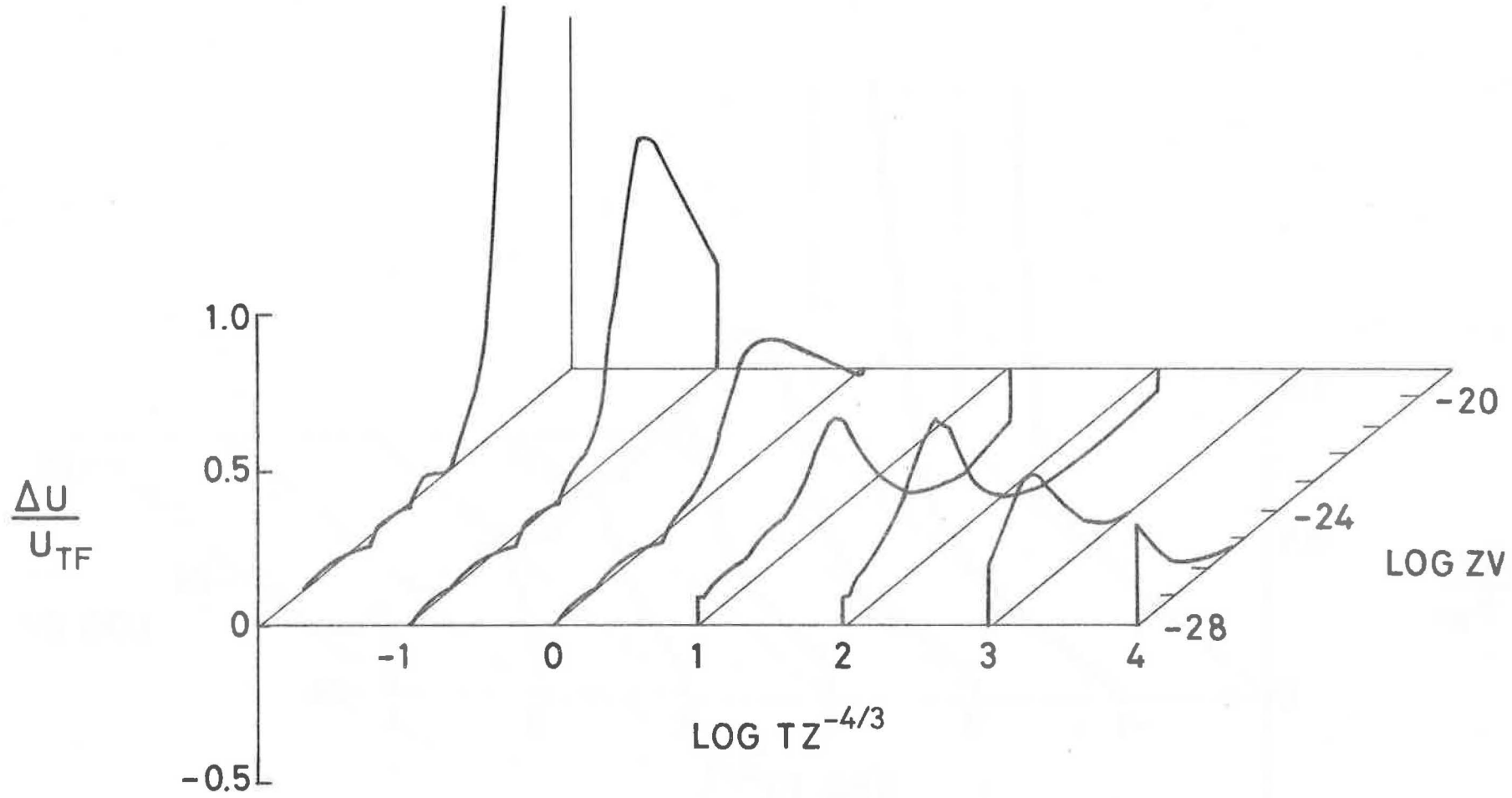

FIG. 6

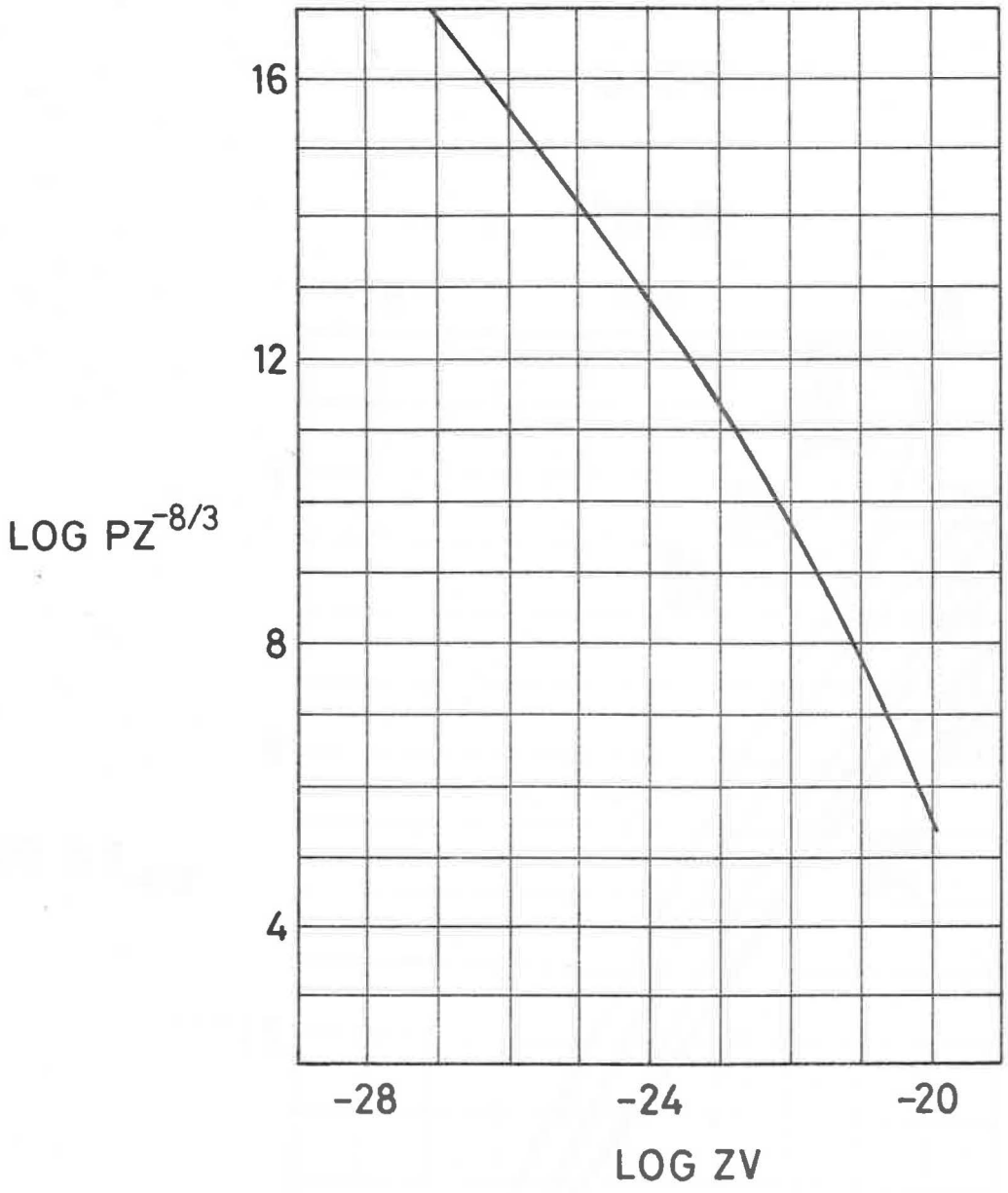

FIG. 7

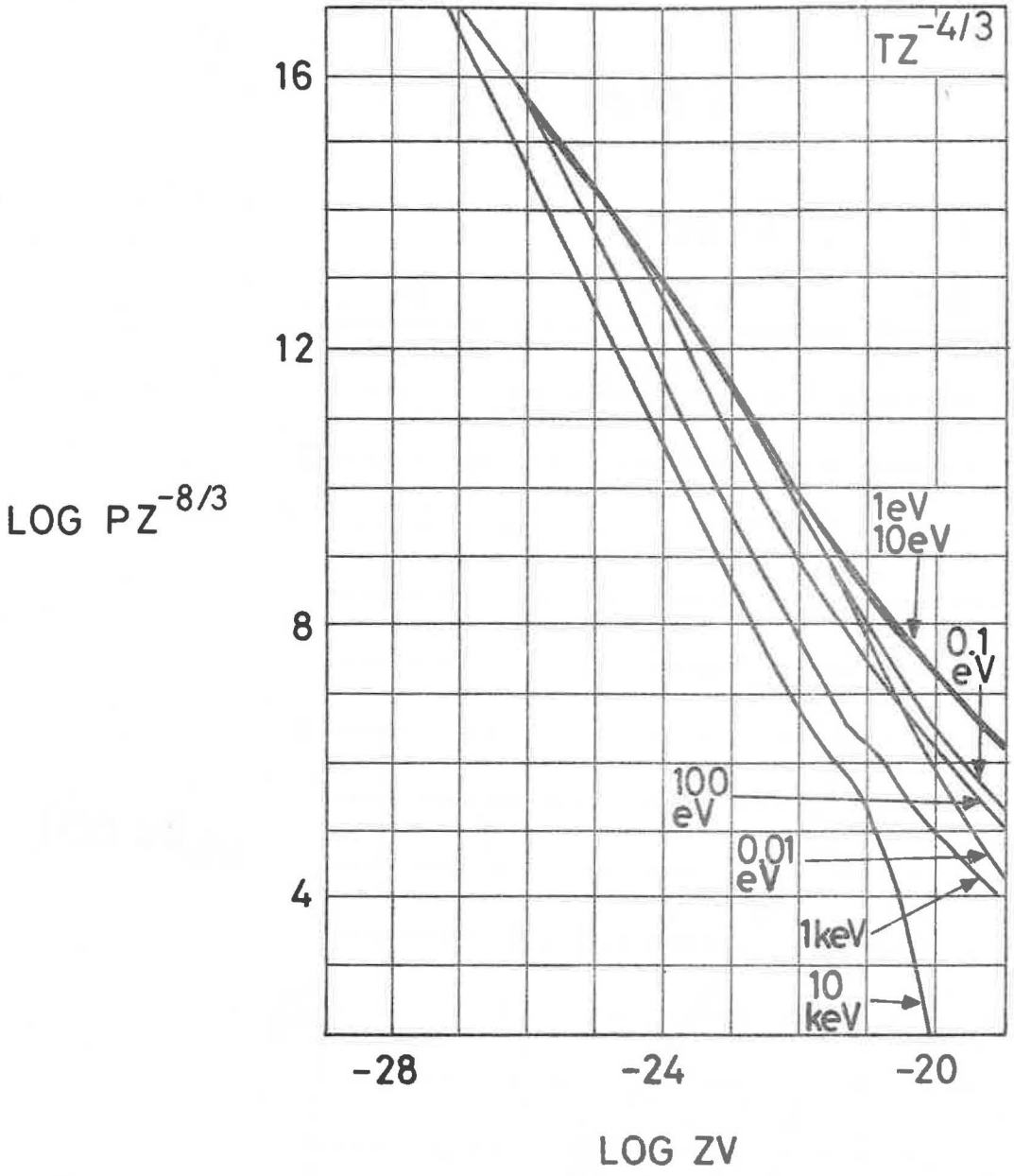
TZ^-4/3
16
12
8
4
LOG PZ^-8/3
1eV
10eV
0.1
eV
100
eV
0.01
eV
1keV
10
keV
-28
-24
-20
LOG ZV

FIG.8

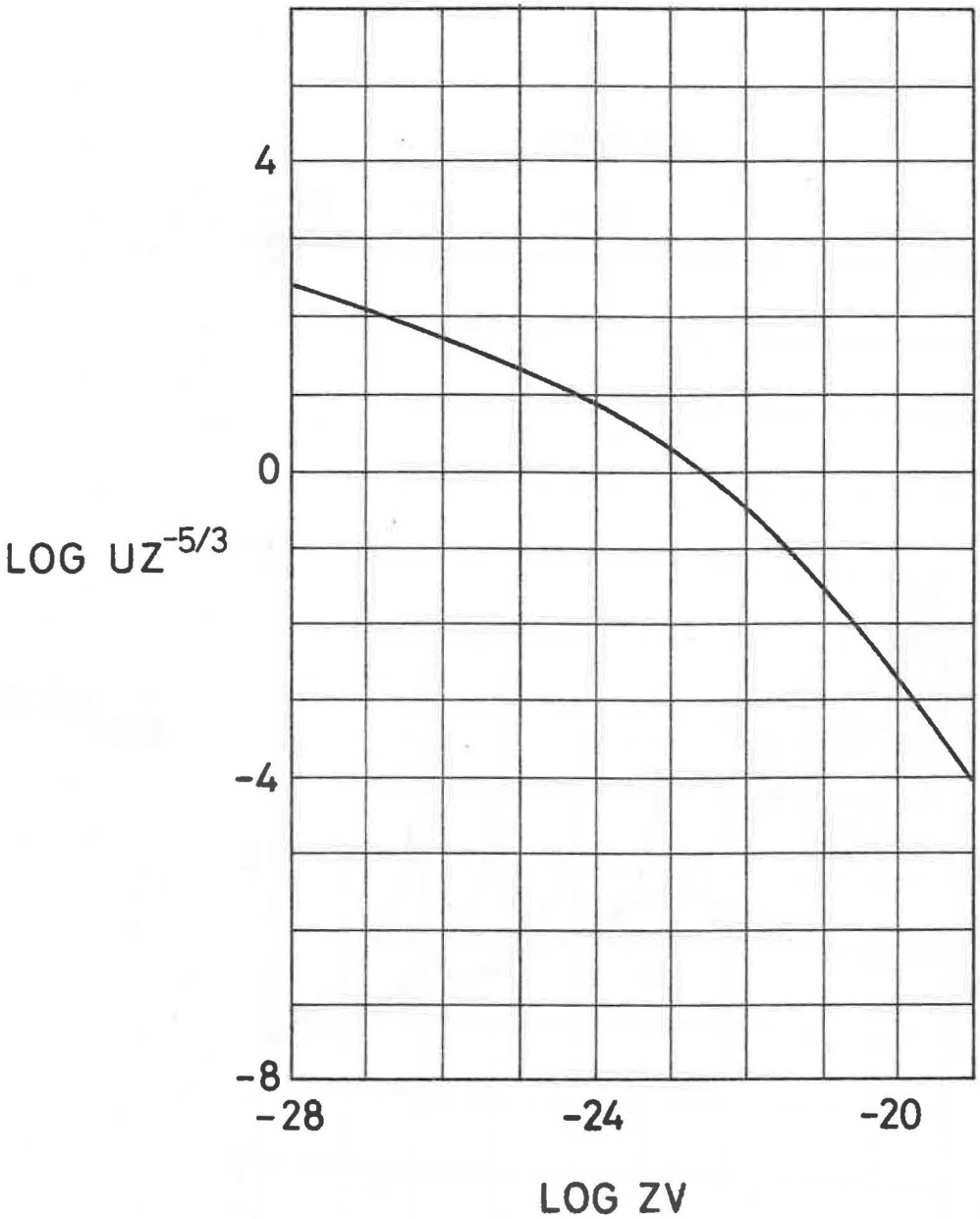

FIG. 9

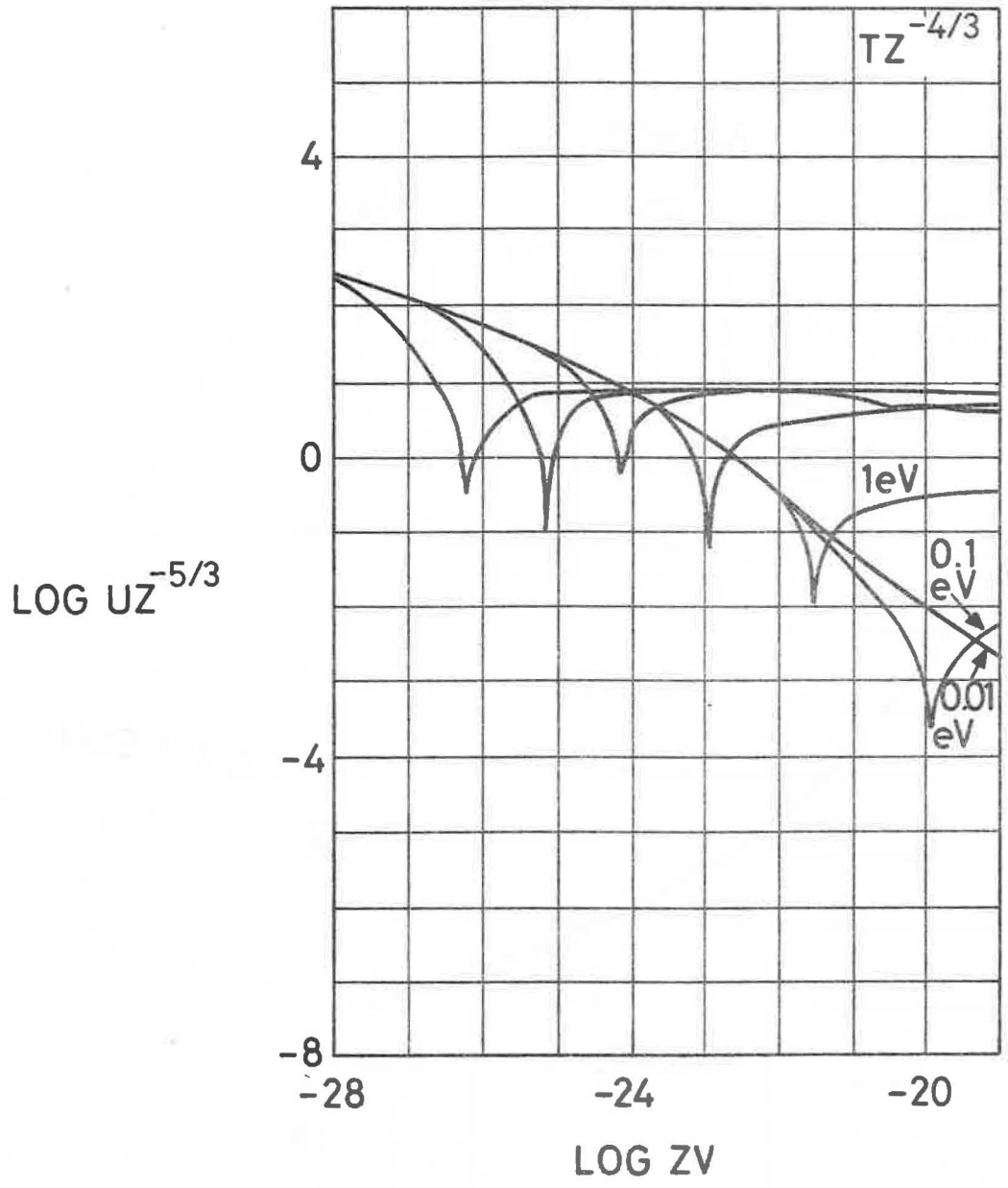

FIG.10

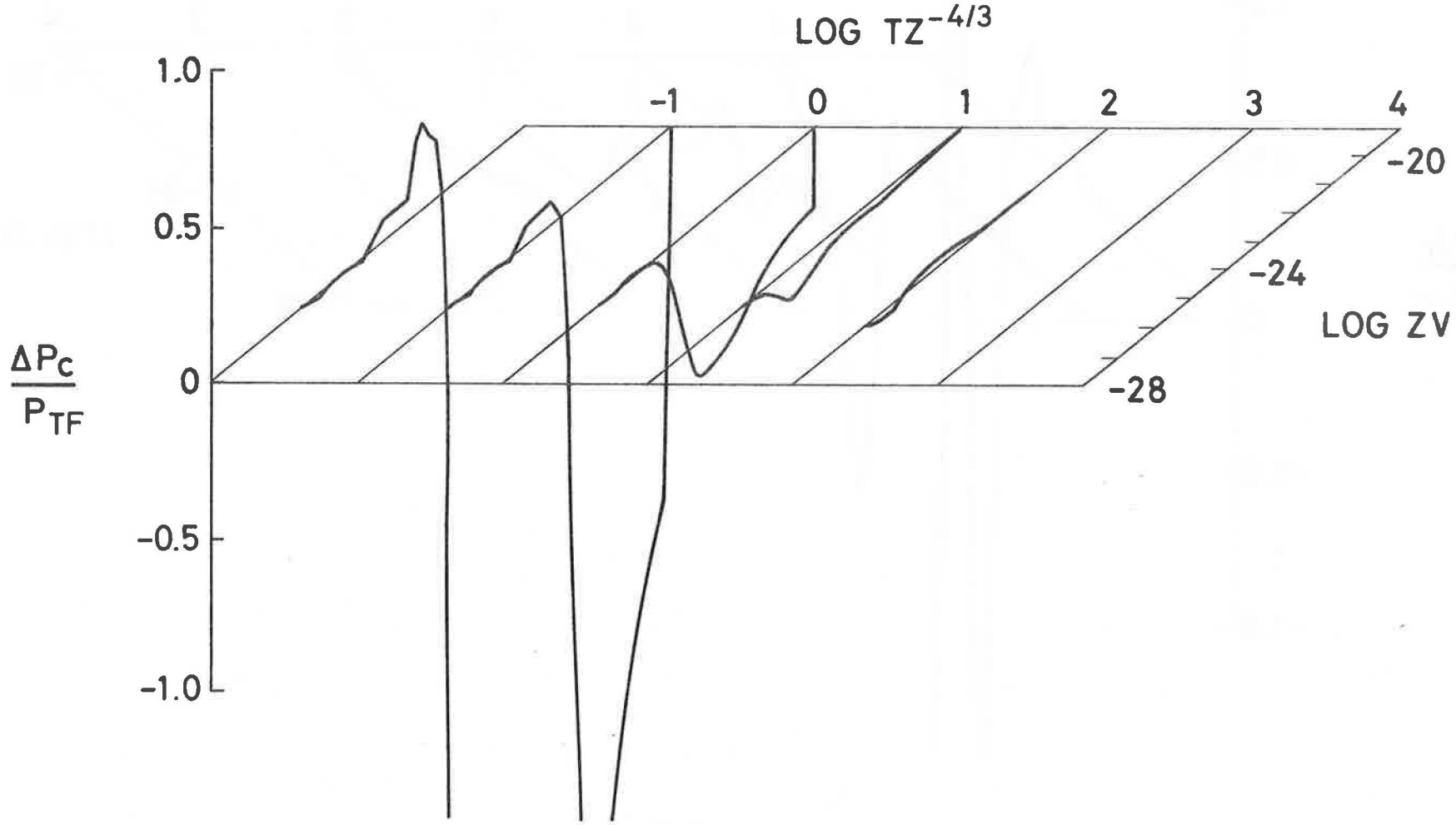

FIG. 11

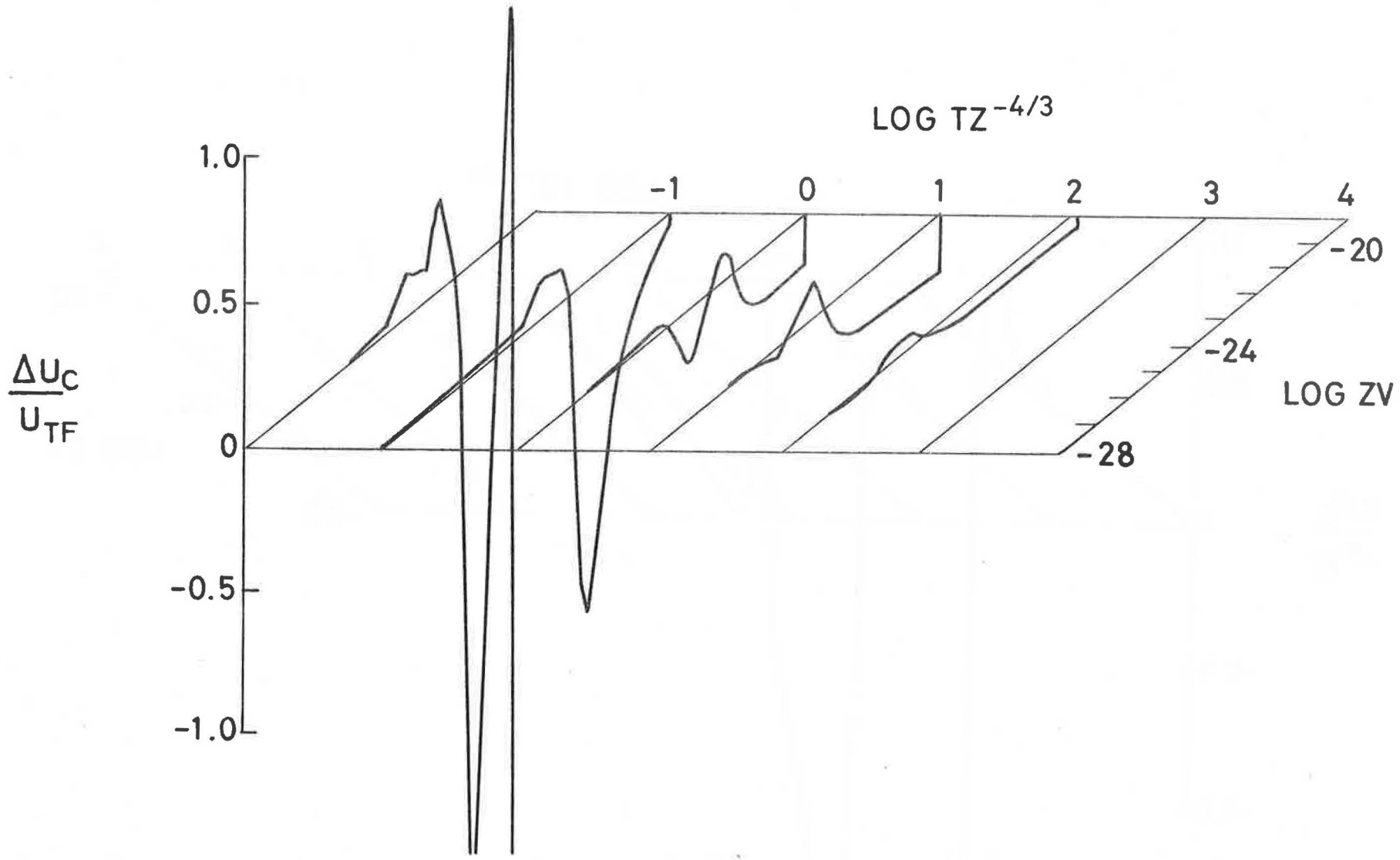

FIG. 12

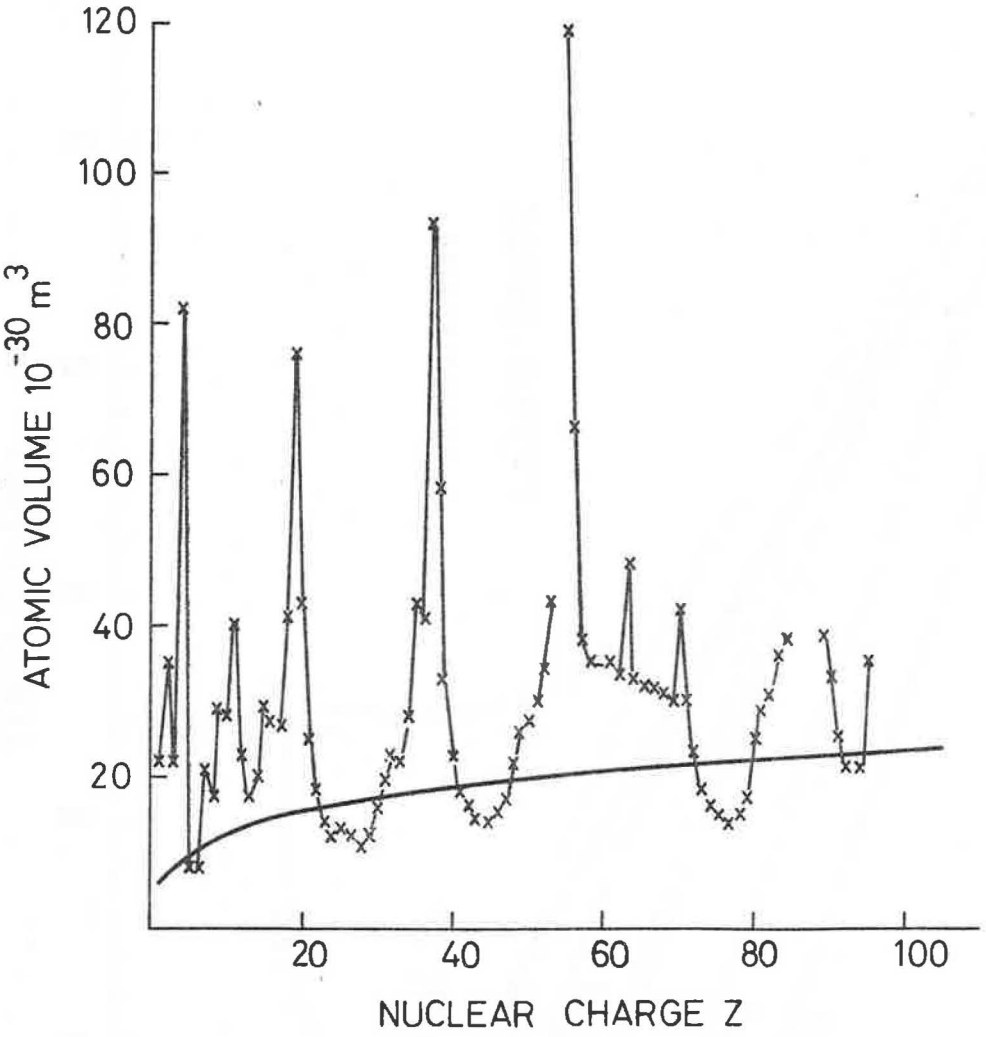
120
100
80
60
40
20
ATOMIC VOLUME 10^{-30} m^3
20
40
60
80
100
NUCLEAR CHARGE Z

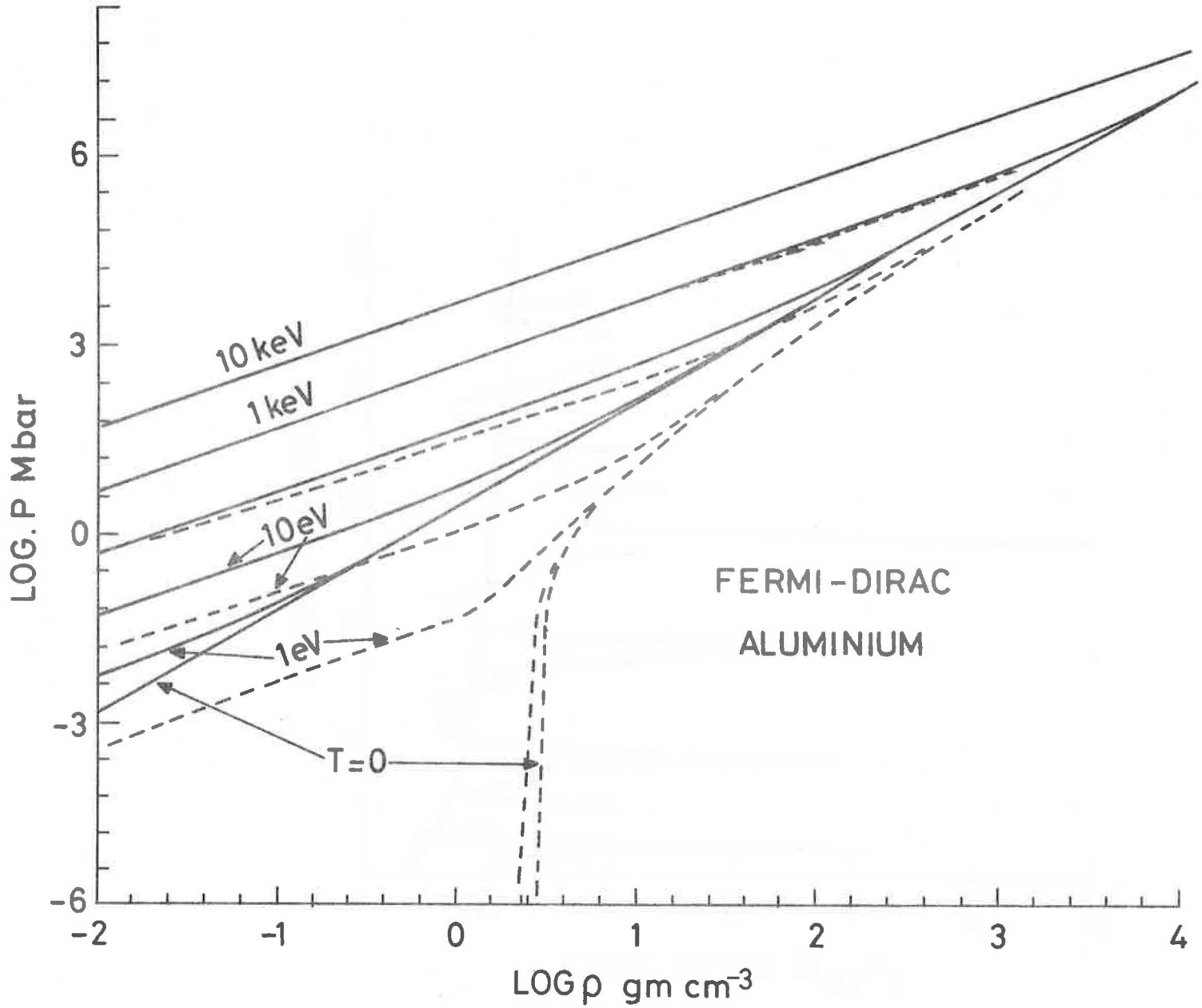
6
3
0
-3
-6
-2
-1
0
1
2
3
4
LOG. P Mbar
LOG ρ gm cm^{-3}
10 keV
1 keV
10eV
1eV
T=0
FERMI-DIRAC
ALUMINIUM

FIG. 14.

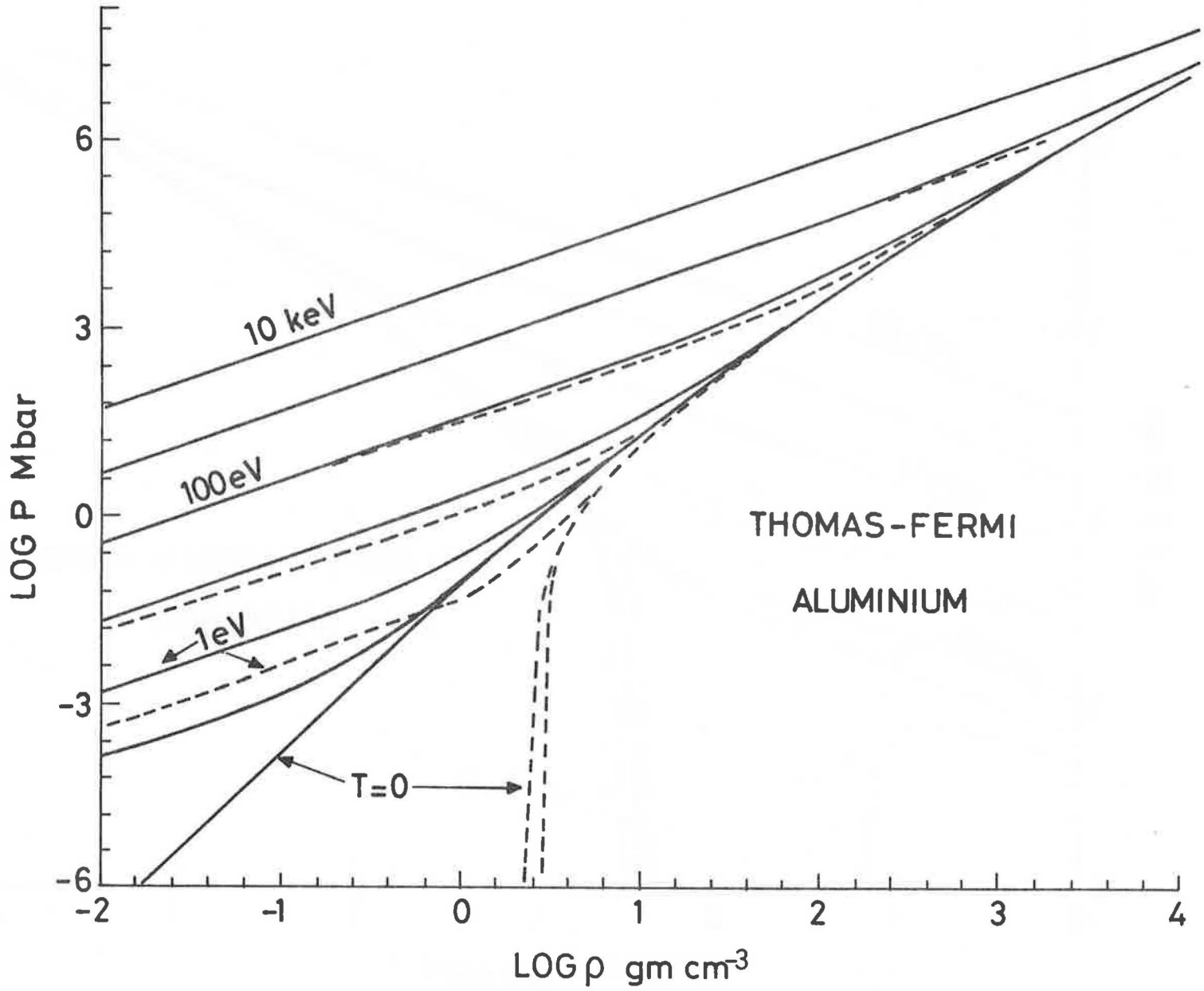
LOG P Mbar
6
3
0
-3
-6
-2
-1
0
1
2
3
4
LOG ρ gm cm-3
10 keV
100eV
1eV
T=0
THOMAS-FERMI
ALUMINIUM

FIG.15

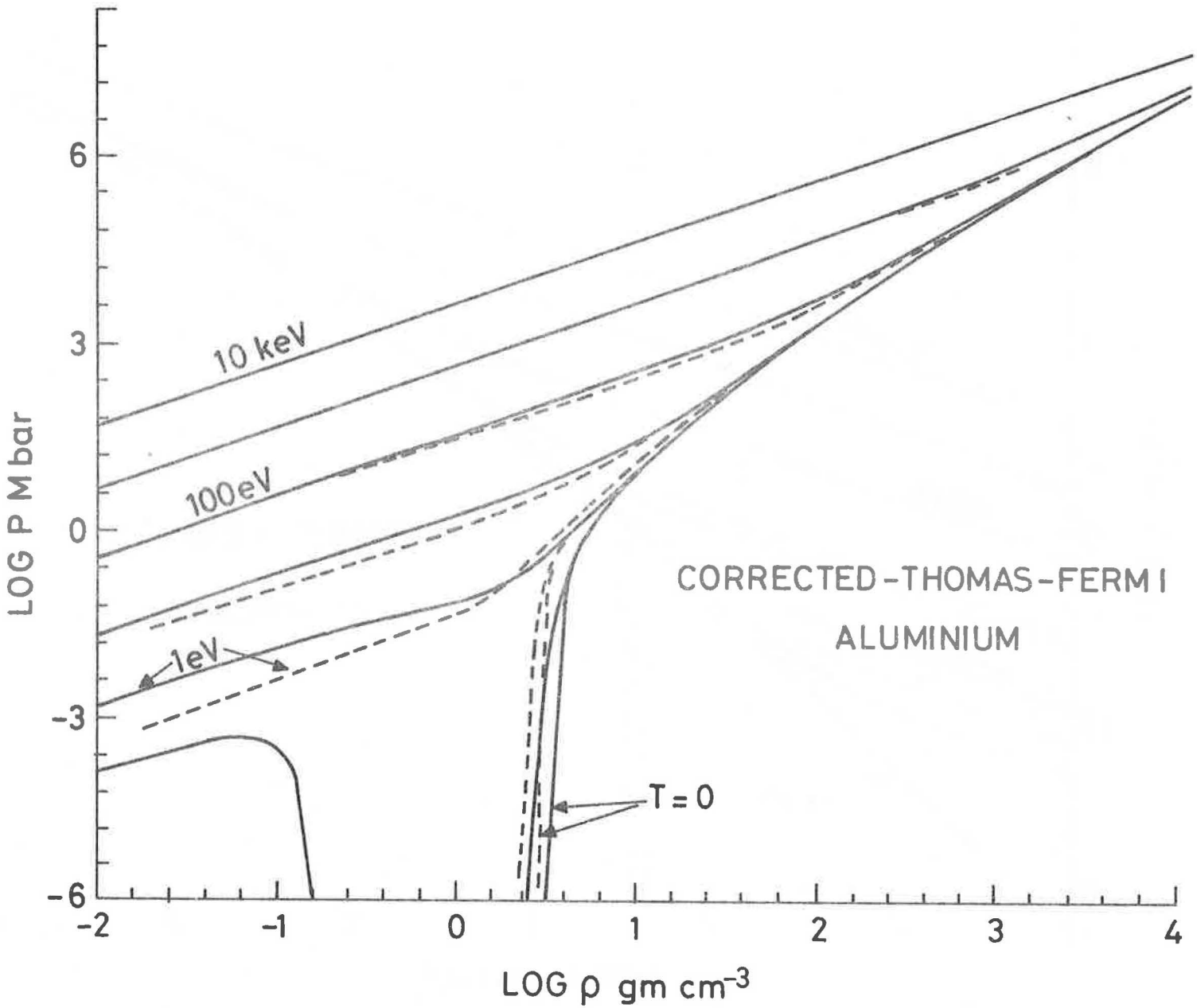
6
3
0
-3
-6
-2
-1
0
1
2
3
4
LOG P M bar
LOG ρ gm cm^{-3}
10 keV
100eV
1eV
T = 0
CORRECTED-THOMAS-FERMI
ALUMINIUM

FIG.16

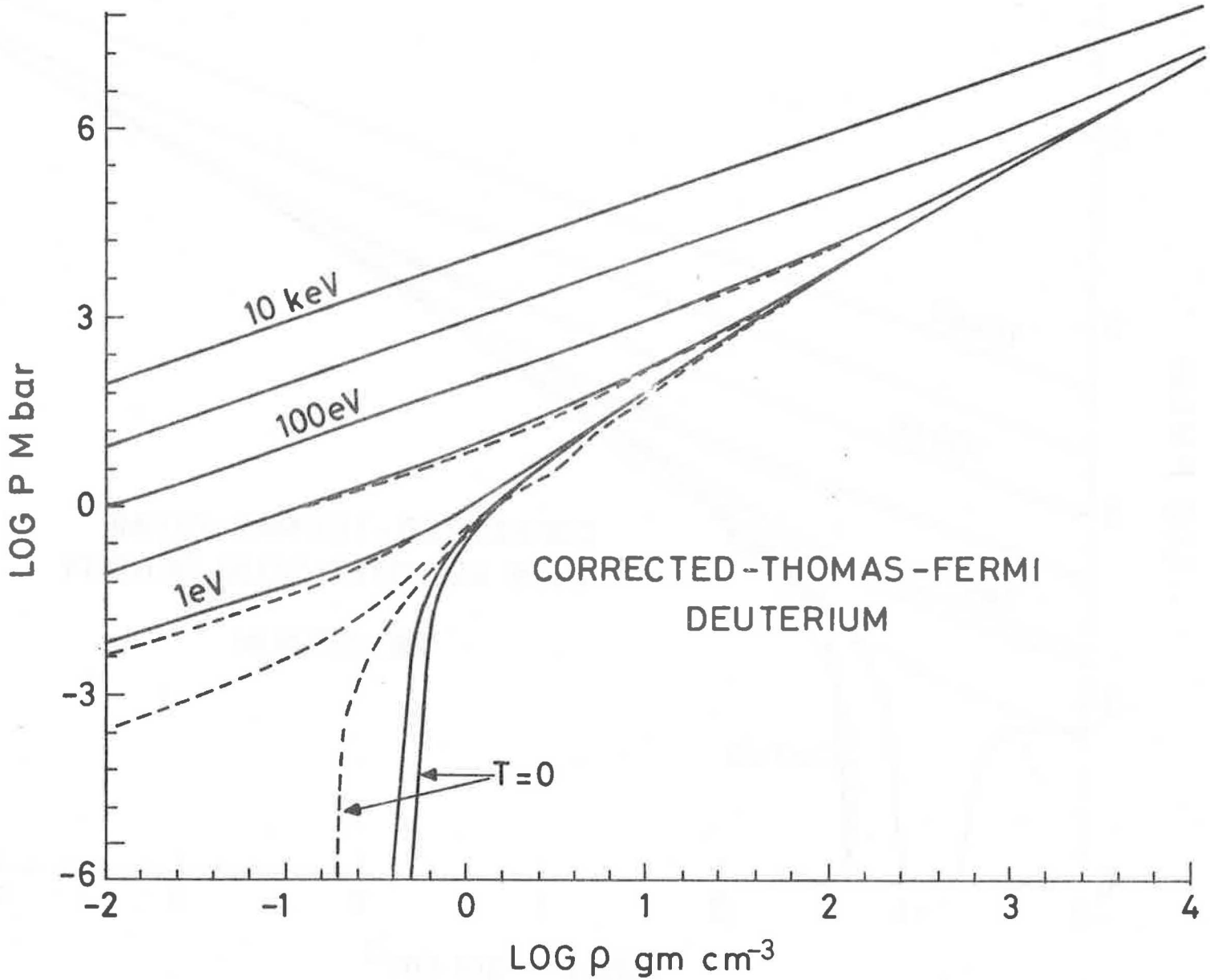
10 keV
100eV
1eV
T=0
CORRECTED-THOMAS-FERMI
DEUTERIUM
LOG P M bar
LOG ρ gm cm^{-3}
6
3
0
-3
-6
-2
-1
0
1
2
3
4

FIG.17.

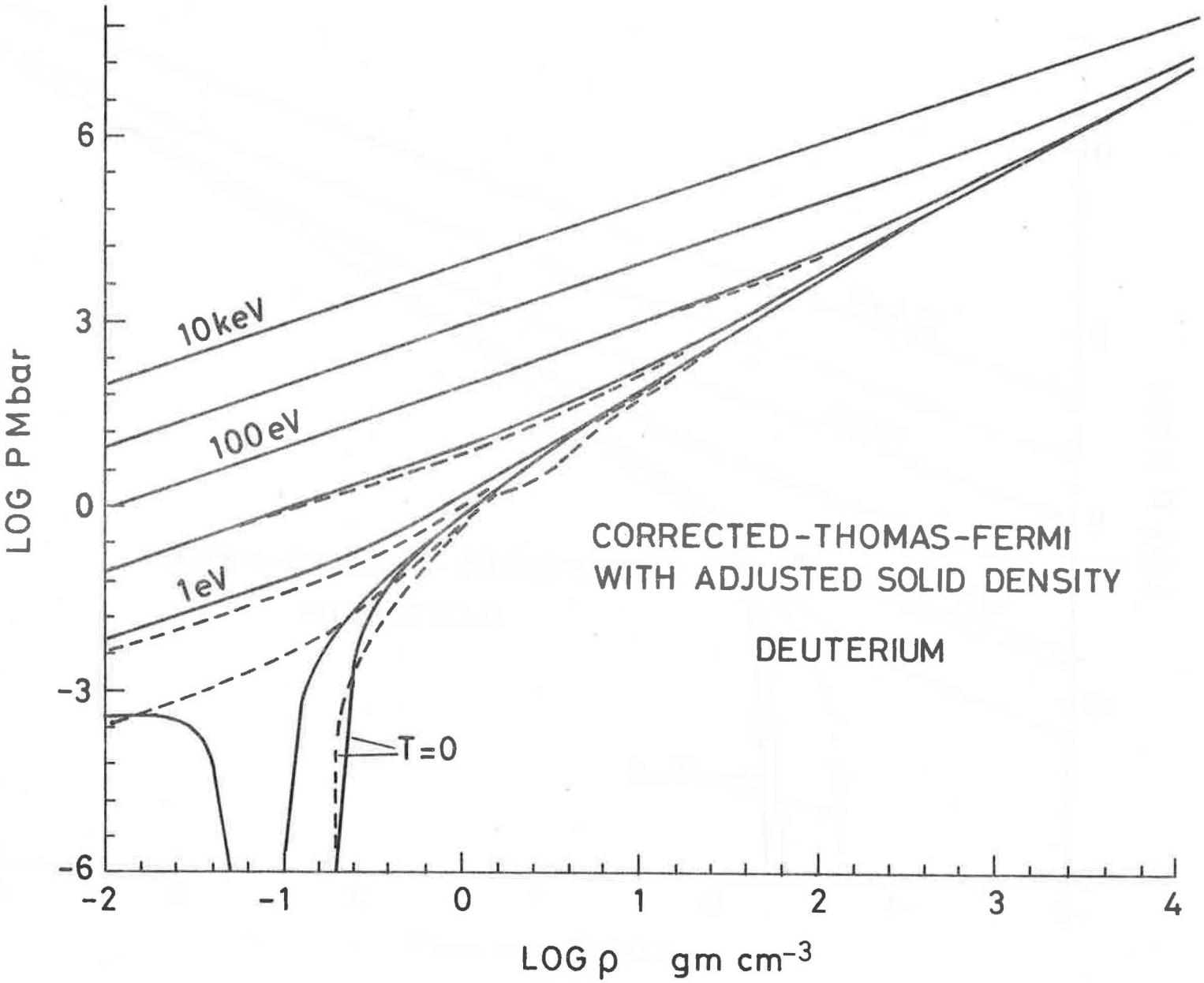
LOG P Mbar
6
3
0
-3
-6
-2
-1
0
1
2
3
4
LOG ρ gm cm^{-3}
10keV
100eV
1eV
T=0
CORRECTED-THOMAS-FERMI
WITH ADJUSTED SOLID DENSITY
DEUTERIUM

FIG.18.